1st Pan-American Congress on Computational Mechanics - PANACM 2015
XI Argentine Congress on Computational Mechanics - MECOM 2015
S. Idelsohn, V. Sonzogni, A. Coutinho, M. Cruchaga, A. Lew & M. Cerrolaza (Eds)

LOCALIZED VERSUS DIFFUSED FAILURE MODES IN CONCRETE SUBJECTED TO HIGH TEMPERATURE

SONIA M. VRECH[1], MARIANELA RIPANI[2] AND GUILLERMO ETSE[3]

[1]CONICET - University of Tucumán
Av. Independencia 1800. 4000 - Tucumán. Argentina
svrech@herrera.unt.edu.ar

[2]CONICET- University of Buenos Aires
Av. Las Heras 2214. C1127AAR - Buenos Aires. Argentina
mripani@fi.uba.ar

[3]CONICET - University of Tucumán
Av. Independencia 1800. 4000 - Tucumán. Argentina
getse@herrera.unt.edu.ar

Key words: Discontinuous bifurcation, gradient poroplasticity, temperature

Abstract. In this work, conditions for discontinuous bifurcation in limit states are derived and evaluated in quasi-brittle materials like concrete, for variable stress states, loading conditions and high temperature scenarios. This is performed in the framework of a thermodynamically consistent non-local poroplastic constitutive theory for quasi-brittle materials subjected to high temperature [14]. Thereby, gradient poroplasticity and fracture energy-based homogenization are combined to describe the post-peak behavior of porous media when subjected to long term exposure of temperature. For the numerical implementation of the model, the consistent tangent operator is developed and the dual mixed FE formulation for thermodynamically consistent gradient plasticity by [20] is considered, which was extended to porous media by [10]. The explicit solutions for brittle failure conditions in the form of discontinuous bifurcation are proposed for this poroplastic constitutive theory based on gradient plasticity. The results provide relevant information regarding the variation of the transition point of brittle-ductile failure mode with the acting temperature and confining pressure.

1 INTRODUCTION

Failure behavior of quasi-brittle materials like concrete is characterized by strong spatial discontinuities of the kinematic fields when they are sufficiently deformed into the inelastic regime, depending on the governing stresses and on the mechanical and chemical features of the material micro and mesostructure, see a.o. [23, 18].

Whereas in tensile regime the concrete response is highly brittle as the damage entirely localizes in one single crack of zero width while the material outside the crack remains practically undamaged and subjected to elastic unloading, see a.o. [13, 3], in compressive regime the ductility of concrete failure behavior strongly increases with the confining pressure, governed by both, fracture energy releases in active microcracks and material degradation in between these cracks, see a.o. [8, 17].

This complex variation from brittle to ductile failure modes depending on the acting stress state, is also strongly affected by variable temperature fields. This effect strongly influences the mechanical behavior and the overall strength capacity of the related structures. Regarding the influence of the concrete performance on its sensitivity to high temperatures, many authors agree that high strength concretes reduce their resistance when they are subjected to high temperatures, see a.o. [1, 5].

Based on the first contributions related to the concrete behavior under high temperatures in porous media framework by [16], and in conjunction with the gradient and fracture energy-based Leon - Drucker Prager (LDP) constitutive model for quasi-brittle materials like concrete by [21], the temperature dependent Leon - Drucker Prager model (TD-LDP) have been formulated by the authors, see [14].

In this work, it becomes particularly important the evaluation of brittle or localized failure modes of poroplastic materials that in the framework of continuums models are described in terms of discontinuous bifurcations or jumps in the velocity gradients.

Several analytical and geometrical attempts have been aimed to capture the onset of localization and to determine both direction and amplitude of the related cracks or shear bands. After the original works by [6, 7], many authors studied the problem in a systematic manner, formulating mathematical indicators that signalize the initiation of localized failure modes in the form of discontinuous bifurcation, see a.o. [23, 12]. In the field of quasi-brittle materials can be cited the contributions by [4, 19, 22]. Recently, discontinuous bifurcation analysis of thermodynamically consistent gradient poroplastic materials have been developed by [11].

Analytical methods are applied in this contribution to evaluate the predictions of localized failure modes and the transition from brittle to ductile failure provided by the thermodynamically consistent gradient and fracture energy-based plasticity theory for poroplastic materials like concrete subject to high temperature levels.

2 THERMODYNAMICALLY CONSISTENT GRADIENT BASED POROPLASTIC THEORY

The First Thermodynamics Law corresponding to poroplastic gradient materials states that

$$\dot{E} + \dot{K} = P + Q \tag{1}$$

with the internal and kinetic energy rates $\dot{E}$ and $\dot{K}$, the mechanic work of external forces P and the externally supplied heat Q are computed as

$$\dot{E} = \frac{\mathrm{d}}{\mathrm{d}t}\int_\Omega e \; \mathrm{d}\Omega; \qquad \dot{K} = \frac{1}{2}\int_\Omega \left[\rho_s \left(1-\phi\right) \dot{\mathbf{u}}_s \cdot \dot{\mathbf{u}}_s + \rho_f \phi \, \mathbf{w} \cdot \mathbf{w}\right] \mathrm{d}\Omega \tag{2}$$

$$P = \int_{\partial\Omega} \left(\boldsymbol{\sigma} \cdot \mathbf{n}_s \cdot \dot{\mathbf{u}}_s - \frac{p}{\rho_f}\mathbf{n}_s \cdot \mathbf{w}\right) \mathrm{d}\partial\Omega + \int_\Omega \rho \, \mathbf{b} \cdot \dot{\mathbf{u}}_s \; \mathrm{d}\Omega \tag{3}$$

$$Q = \int_\Omega \rho r \; \mathrm{d}\Omega - \int_{\partial\Omega} \mathbf{h} \cdot \mathbf{n}_s \; \mathrm{d}\partial\Omega \tag{4}$$

being $e = e_s + e_f$ the internal energy density, where the subscripts s and f denote the skeleton and fluid components respectively, $\mathbf{w}$ the fluid mass flux vector, $\rho = \rho_s(1-\phi)+\rho_f\phi$ the total density of the body and ϕ, the porosity. Moreover $\mathbf{u}_s$ represents the velocity vector of the skeleton, $\boldsymbol{\sigma}$ the total Cauchy tensor, $\mathbf{b}$ the body forces, r the applied heat sources, p the pore pressure and $\mathbf{h}$ the heat flux vector.

The Second Thermodynamics Law is expressed as

$$\dot{S} - Q_T \geq 0 \tag{5}$$

being $\dot{S}$ the system entropy rate and Q_T the entropy flux. Each term in Eq. (5) is defined as

$$\dot{S} = \int_\Omega \left[\rho \dot{s} + \nabla \cdot \left(s_f^m \mathbf{w}\right)\right] \mathrm{d}\Omega; \qquad Q_T = -\int_{\partial\Omega} \frac{\mathbf{h} \cdot \mathbf{n}_s}{T} \mathrm{d}\partial\Omega + \int_\Omega \frac{\rho r}{T} \mathrm{d}\Omega \tag{6}$$

being s the internal entropy density, s_f^m the fluid internal entropy per unit of mass and T the absolute temperature. According to [2], the weak form of the Second Thermodynamics Law can be obtained as

$$\int_\Omega \left[\boldsymbol{\sigma} : \dot{\boldsymbol{\varepsilon}} + g_f^m \dot{m} + \rho T \dot{s} - \rho \dot{e} + \mathbf{w} \cdot \left(\nabla s_f^m - \nabla h_f\right) - \frac{\mathbf{h}}{T} \cdot \nabla T\right] \mathrm{d}\Omega \geq 0 \tag{7}$$

where g_f^m is the enthalpy density per unit mass, $h_f = e_f^m + p/\rho_f$ corresponds to the fluid specific enthalpy, e_f^m is the fluid internal energy per unit of mass and $\boldsymbol{\varepsilon}$ is the strain tensor.

Regarding Eq. (7) and taking into account that an arbitrary thermodynamic states of an open gradient poroplastic material under non-isothermal condition may be defined in terms of the elastic strain tensor $\boldsymbol{\varepsilon}^e = \boldsymbol{\varepsilon} - \boldsymbol{\varepsilon}^p$, the elastic fluid mass content $m^e = m - m^p$, the elastic entropy $s^e = s - s^p$ and the scalar internal variable q, in case of isotropic plasticity, the Coleman's equations result

$$\boldsymbol{\sigma} = \rho \frac{\partial \psi_s}{\partial \boldsymbol{\varepsilon}^e} \quad , \quad p = \rho \rho_f \frac{\partial \psi_s}{\partial m^e} \quad , \quad s_s = -\frac{\partial \psi_s}{\partial T} \tag{8}$$

$$Q^l = -\rho \frac{\partial \psi_s}{\partial q} \quad , \quad Q^{nl} = T \nabla \cdot \left(\frac{\rho}{T} \frac{\partial \psi_s}{\partial \nabla q}\right) \quad \text{in the domain } \Omega \tag{9}$$

Whereas the dissipations related to the plastic process, heat and fluid mass transports can be computed as

$$\varphi^p = \boldsymbol{\sigma} : \dot{\boldsymbol{\varepsilon}}^p + \frac{p}{\rho_f}\dot{m}^p + Q\dot{q} \geq 0; \quad \varphi^{th} = -\frac{\mathbf{h}\cdot\nabla T}{T} \geq 0; \quad \varphi^f = \mathbf{w}\cdot\left(\nabla s_f^m - \nabla h_f\right) \geq 0 \quad (10)$$

To achieve the above equations from Eq. (7), it is assumed that the total Helmholtz's free energy is decomposed as $\psi = e - Ts = \psi_s + m\,\psi_f$ and the total entropy is decomposed $s = s_s + m\,s_f$, where ψ_s and ψ_f are the solid- and the fluid-specific Helmholtz's free energy respectively, s_s and s_f are the specific entropies related to the solid skeleton and the fluid part respectively, and $Q = Q^l + Q^{nl}$ is the total dissipative stresses, with Q^l the local dissipative stress and Q^{nl} the non-local gradient one.

Adopting the following additive expression for the Helmholz's free energy

$$\psi_s\left(\boldsymbol{\varepsilon}^e, m^e, T, q, \nabla q\right) = \psi^e\left(\boldsymbol{\varepsilon}^e, m^e, T\right) + \psi^l\left(q, T\right) + \psi^{nl}\left(\nabla q\right), \quad (11)$$

the elastic, local and non-local plastic counterparts of the free energy are given by

$$\rho\psi^e = \frac{1}{2}\boldsymbol{\varepsilon}^e : \mathbf{E} : \boldsymbol{\varepsilon}^e + \frac{1}{2}M\left(\frac{m^e}{\rho_f}\right)^2 - \frac{1}{2}\chi T^2 + \aleph m^e T - \frac{m^e}{\rho_f}M\mathbf{B} : \boldsymbol{\varepsilon}^e - T\mathbf{A} : \boldsymbol{\varepsilon}^e \quad (12)$$

$$\rho\psi^l = \frac{H}{2}q^2 - Ts_{fr}^{(q)}; \qquad \rho\psi^{nl} = \frac{1}{2}l_c^2\,\nabla q \cdot \mathbf{H}^{nl} \cdot \nabla q \quad (13)$$

being $\mathbf{E}$ the fourth order elastic tensor, M the Biot's modulus, χ the concrete heat capacity, $\aleph$ the latent heat of variation in fluid mass content, $\mathbf{B} = b\mathbf{I}$ the Biot's tensor with b the Biot's coefficient and $\mathbf{I}$ the second order identity tensor, and $\mathbf{A} = \alpha_T\mathbf{I}$ the thermal expansion tensor, with α_T the thermal expansion coefficient.

In Eq. (13-a), $s_{fr}^{(q)}$ represents the unrecovered entropy called frozen entropy, see [2]. Moreover, in Eq. (13-b) H is the local-plastic hardening/softening modulus, $\mathbf{H}^{nl}$ the gradient softening second-order tensor and l_c the gradient characteristic length. In the particular case of gradient isotropy, the gradient softening second-order tensor can be expressed as $\mathbf{H}^{nl} = H^{nl}\mathbf{I}$, being H^{nl} a positive non-zero scalar.

2.1 Constitutive equations

Summarizing, the constitutive equations in terms of total stresses, pore pressure, fluid-specific internal entropy and dissipative stresses for thermodynamically consistent gradient poroplastic materials subjected to non-isothermal conditions are

$$\boldsymbol{\sigma} = \mathbf{E} : \boldsymbol{\varepsilon}^e - M\frac{m^e}{\rho_f}\mathbf{B} - T\mathbf{A} \quad (14)$$

$$p = \frac{M}{\rho_f}m^e - M\mathbf{B} : \boldsymbol{\varepsilon}^e + \rho_f\aleph T; \qquad s_s = \mathbf{A} : \boldsymbol{\varepsilon}^e - \aleph m^e + \chi T + s_{fr}^{(q)} \quad (15)$$

$$Q^l = -Hq + T\frac{\partial s_{fr}^{(q)}}{\partial q}; \qquad Q^{nl} = l_c^2 H^{nl}\left(-\frac{\nabla T}{2T}\cdot\nabla q + \nabla^2 q\right) \quad (16)$$

2.2 Non-local poroplastic flow rule

For general non-associated flow rule and hardening/softening laws, the yield surface Φ and the dissipative potential Φ^* are introduced. The rate of the plastic strains tensor, plastic mass and internal variables are defined as

$$\dot{\boldsymbol{\varepsilon}}^p = \dot{\lambda}\frac{\partial \Phi^*}{\partial \boldsymbol{\sigma}} \quad , \quad \dot{m}^p = \dot{\lambda}\frac{\partial \Phi^*}{\partial p} \quad , \quad \dot{q} = \dot{\lambda}\frac{\partial \Phi^*}{\partial Q} \tag{17}$$

being $\dot{\lambda}$ the rate of the plastic multiplier. To complete the problem formulation, the Kuhn-Tucker conditions and poroplastic consistency must be introduced (See a detailed explanation in [14])

$$\dot{\lambda} \geq 0 \quad , \quad \Phi(\boldsymbol{\sigma}, p, Q) \leq 0 \quad , \quad \dot{\lambda}\Phi(\boldsymbol{\sigma}, p, Q) = 0 \qquad ; \qquad \dot{\Phi} = 0 \tag{18}$$

3 SOLUTIONS FOR LOCALIZED FAILURE OF POROUS MEDIA

In the realm of the smeared crack approach, localized failure modes are related to discontinuous bifurcations of the equilibrium path, and lead to lost of ellipticity of the equations that govern the static equilibrium problem. Analytical solutions of the discontinuous bifurcation condition in gradient non-local continua has been performed by [15], whereas bifurcation analysis in gradient-based poroplastic media has been carried out by [9], establishing the discontinuous bifurcation condition as either the jump of the velocity gradients

$$[\dot{u_{i,j}}] = c_i n_j \quad , \quad [\dot{\varepsilon}_{ij}] = \frac{1}{2}\left(c_i n_j + n_j c_i\right) \tag{19}$$

being n_i the unit vector normal to the characteristic failure surface S, and/or the jump of the rate of fluid mass content

$$[\dot{m}] = -M_{i,i} = -n_i c_i^M \tag{20}$$

different to zero. Moreover, the following balance conditions must be considered, see [6, 2]

$$c[p_{,i}] + [\dot{p}]n_i = 0; \qquad c[\sigma_{ij,j}] + [\dot{\sigma}_{ij}]n_j = 0 \tag{21}$$

being c the discontinuous propagation velocity.

3.1 Bifurcation analysis in drained local porous media

Regarding the drained state in a hardened concrete, taking into account Eq. (21-b) and the evolution of the constitutive equation in Eq. (14), the following condition is obtained

$$[\dot{\sigma}_{ij}]n_j = Q_{ij}c_j = 0 \tag{22}$$

where Q_{ij} is the elastoplastic acoustic tensor for local poroplasticity under drained conditions, computed as

$$Q_{ij} = E^{ep}_{ijkl} n_l n_k = Q^e_{ij} - Q^p_{ij} \tag{23}$$

with E^{ep}_{ijkl} the solid skeleton elastoplastic tensor, $Q^e_{ij} = E_{ijkl} n_l n_k$ the elastic component of the acoustic tensor, and

$$Q^p_{ij} = \frac{E_{ijmn} f^*_{mn} f_{pq} E_{pqkl}}{h} n_l n_k \quad \text{with} \quad f^*_{mn} = \frac{\partial \Phi^*}{\partial \sigma_{mn}} \quad , \quad f_{pq} = \frac{\partial \Phi}{\partial \sigma_{pq}} \tag{24}$$

the plastic one, being h the generalized plastic modulus (see [10] for detailed explanation).

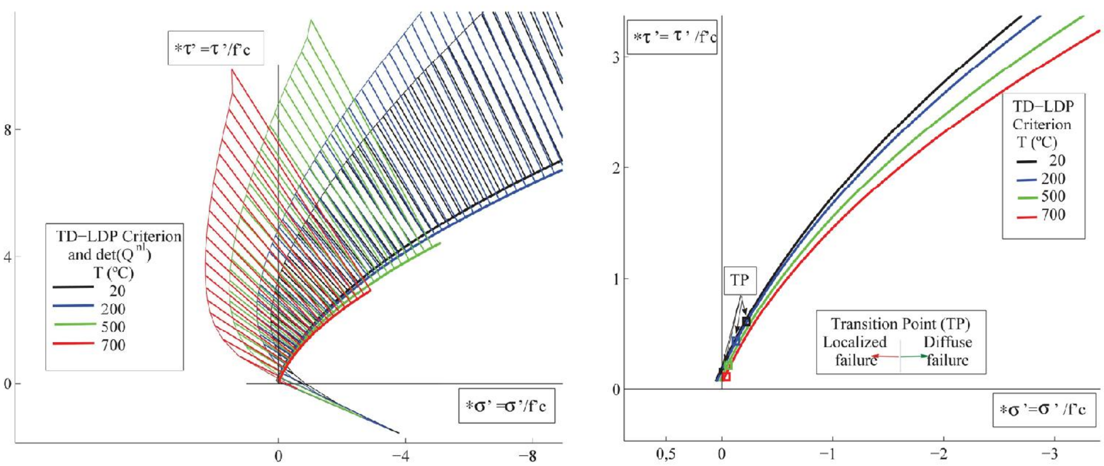

(a) (b)

Figure 1: (a) Localization indicator in normal direction to the TD-LDP maximal strength criterion and (b) Transition points for TD-LDP maximal strength criterion.

3.2 Bifurcation analysis in drained gradient non-local porous media

Analytical solutions of the discontinuous bifurcation conditions in gradient non-local continua follows from the waves propagation analysis, see [15].

Regarding an homogeneous state before the start of the bifurcation, harmonic perturbations to the incremental field variables, i.e. displacements, mass content, plastic multiplier and temperature are applied, representing the propagation of stationary planar waves

$$\begin{pmatrix} \dot{u} \\ \dot{\gamma} \\ \dot{\lambda} \\ \dot{T} \end{pmatrix} = \begin{pmatrix} \dot{U}(t) \\ \dot{\Gamma}(t) \\ \dot{L}(t) \\ \dot{T}(t) \end{pmatrix} \exp\left(\frac{i2\pi}{\delta} \boldsymbol{n} \cdot \boldsymbol{x}\right) \tag{25}$$

being $\dot{\gamma}$ the mass content rate, $\boldsymbol{x}$ the position vector (in Cartesian coordinates) and δ the wave length. The wave solutions are represented by $\dot{U}(t)$, $\dot{\Gamma}(t)$, $\dot{L}(t)$ and $\dot{T}(t)$.

Considering Eq. (25) together with equilibrium condition on the discontinuity surface and plastic consistency condition for gradient plasticity, the solution for drained conditions results

$$\left(\frac{2\pi}{\delta}\right)^2 \left[E_{ijkl} - \frac{E_{ijmn} f^*_{mn} f_{pq} E_{pqkl}}{h + h^{nl}}\right] n_l n_k \dot{U} = 0 \tag{26}$$

being h^{nl} the generalized gradient modulus. Equation (26) leads to the expression of the acoustic tensor for non-local gradient plasticity under drained conditions

$$Q^{nl} = E_{ijkl} - \frac{E_{ijmn} f^*_{mn} f_{pq} E_{pqkl}}{h + h^{nl}} \tag{27}$$

The localized failure condition; $\det\left(Q^{nl}\right) = 0$, leads to the analysis of the spectral properties of the localization tensor. Moreover, analytical solutions of the acoustic tensor's eigenvalues and eigenvector problem leads to explicit solutions of critical hardening/softening modulus

$$H_{crit} = n_i E_{ijkl} {f^*}_{kl} P_{jm} f_{no} E_{nomq} n_q - f_{ij} E_{ijkl} {f^*}_{kl} \quad \text{being} \quad \boldsymbol{P} = \boldsymbol{Q}^{-1} \tag{28}$$

as well as critical localization angles θ_i, that define the localization directions $\boldsymbol{n}$, normal to the failure surface S.

4 GRADIENT- AND FRACTURE ENERGY-BASED TEMPERATURE DEPENDENT LEON-DRUCKER PRAGER CONSTITUTIVE MODEL

The fracture energy-based temperature dependent Leon-Drucker Prager (TD-LDP) constitutive model for concrete has been proposed by [14] in the framework of the thermodynamically consistent gradient-based theory for poroplastic materials.

The maximum strength criterion

$$\Phi({}^*\sigma', {}^*\tau, T) = \alpha(T)\,\frac{3}{2}\,{}^*\tau^2 + \beta(T)\, m_0 \left(\frac{{}^*\tau}{\sqrt{6}} + {}^*\sigma'\right) - c_0 = 0 \tag{29}$$

is defined in the space of effective stresses to account for the poromechanical material description

$$\sigma' = \frac{I_1}{3} - p \quad ; \quad \tau = \sqrt{2J_2} \quad \rightarrow \quad {}^*\sigma' = \frac{\sigma'}{f'_c} \quad ; \quad {}^*\tau = \frac{\tau}{f'_c} \tag{30}$$

being σ' and τ the Haigh Westergaard effective volumetric and deviatoric stress coordinates, respectively, I_1 the first invariant of total stress tensor, J_2 the second invariant of deviatoric stress tensor, and f'_c and f'_t the uniaxial compressive and tensile strengths, respectively. The friction and cohesion of the virgin material, m_0 and c_0, are calibrated at room temperature. The temperature-dependent functions $\alpha(T)$ and $\beta(T)$ vary according to

$$\alpha(T) = (1-\gamma_1 T)^{(-1)} \quad ; \quad \beta(T) = (1-\gamma_2 T)\,(1-\gamma_1 T)^{(-1)} \tag{31}$$

being γ_1 and γ_2 coefficients to be calibrated depending on the concrete quality.

To capture the diverse inelastic behaviors, one single equation-based yield surface is proposed

$$\Phi(^*\sigma, {}^*\tau, T, {}^hQ, {}^sQ) = \alpha(T)\,\frac{3}{2}{}^*\tau^2 + {}^hQ\,\beta(T)\,m_0\left(\frac{{}^*\tau}{\sqrt{6}} + {}^*\sigma'\right) - {}^hQ\,{}^sQ = 0 \qquad (32)$$

Whereas the adopted plastic potential surface yields

$$\Phi^*(^*\sigma, {}^*\tau, T, {}^hQ, {}^sQ) = \alpha(T)\,\frac{3}{2}{}^*\tau^2 + \beta(T)\,m_0\left(\frac{{}^*\tau}{\sqrt{6}} + \eta\,{}^*\sigma'\right) - {}^hQ\,{}^sQ = 0 \qquad (33)$$

being η the volumetric non-associativity degree which varies between $0 \leq \eta \leq 1$.

The evolution of the yield and plastic potential surfaces in pre-peak regime is controlled by the hardening dissipative stress ${}^hQ_0 \leq {}^hQ \leq 1$, while the softening dissipative stress remains constant ${}^sQ = 1$. When ${}^hQ = 1$ the TD-LDP criterion is reached.

Softening behavior of concretes under high temperatures is related to deformation processes under increasing inhomogeneities. The strength degradation during softening regime, when ${}^hQ = 1$, is defined by the evolution of ${}^sQ$ which continuously reduces as the local and non-local decohesion process develops from its maximum value down to ${}^sQ = 0$.

Two parallel mechanisms contribute to the instantaneous concrete strength in softening regime: the remaining strength for further fracture development in the active cracks, which is defined by a temperature dependent fracture energy-based mechanism, and the remaining strength for further mechanical/thermal degradations in the material in between cracks. The last one is defined by a gradient-based mechanism as ${}^s\dot{Q}^{nl} = -l_c^2 H^{nl} \nabla^2 \dot{\lambda}$. The gradient thermo-plastic characteristic length l_c, which defines the width of the degraded material between active cracks, depends on the temperature level and acting confining pressure (see [14] for detailed explanation).

5 DISCONTINUOUS BIFURCATION SOLUTIONS FOR THE TD-LDP CONSTITUTIVE MODEL

The localization analysis of the thermodynamically consistent TD-LDP constitutive model considers the particular plane strain conditions when $\sigma_z = \nu(\sigma_x + \sigma_y)$. The following material properties are considered

$$\begin{aligned}
\text{Elastic modulus - E} &= 19305.3 \quad MPa \\
\text{Poisson's ratio - } \nu &= 0.2 \\
\text{Uniaxial compressive strength - } f_c' &= 22.0 \quad MPa \\
\text{Uniaxial tensile strength - } f_t' &= 2.7 \quad MPa \\
\text{Initial internal length - } l_{c,i} &= 25.0 \quad mm \\
\text{Maximal internal length - } l_{c,m} &= 110.0 \quad mm \\
\text{Gradient modulus - } H^{nl} &= 470.70 \; MPa
\end{aligned}$$

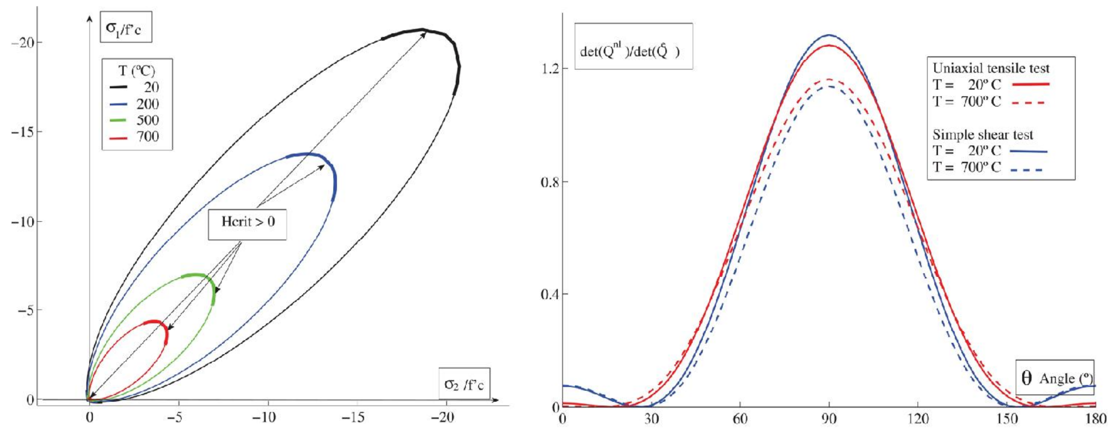

(a) (b)

Figure 2: (a) Critical hardening parameter along TD-LDP maximal strength criterion and (b) Numerical localization analysis with the TD-LDP criterion at peak of the uniaxial tensile and simple shear tests.

In first place, the variation of the normalized localization indicator $\det(Q^{nl})/\det(Q)$ along the maximal strength criterion defined in terms of the normalized first and second Haigh-Westergaard stress coordinates and regarding variable temperature levels from 20°C to 700°C are shown in Fig. 1-a. Transition points (TP) from ductile or diffuse failure modes to brittle or localized ones with variable temperature levels are highlighted in Fig. 1-b. It can be noted that TP move towards the low confinement and tensile regimes with increasing temperature levels.

This transitions are signalized by the appearance of null values of the normalized localization indicator corresponding to discontinuous bifurcation as can be seen in Fig. 1-a. With increasing temperature levels, model predictions realistic reproduces the displacement of the transition point towards lower confinement zones.

The evaluation of the critical hardening parameter H_{crit} has been performed along the entire failure surface in the principal stress space σ_1/f'_c and σ_2/f'_c, regarding variable temperature levels from 20°C to 700°C. Figure 2-a highlights the regions where localized failure modes may occur. The increase of the temperature level influences in the yield condition and destabilizes the failure modes. The results in Fig. 2-a demonstrate that the non-local TD-LDP constitutive model signalizes discontinuous bifurcation in the pre-peak regimes of stress paths in the low confinement region. High temperatures make the situation more critical.

In first place, normalized localization indicators [$\det(Q^{nl})/\det(Q^e)=0$] have been numerically evaluated at the peak stresses corresponding to the simple shear, uniaxial tensile, uniaxial compression and triaxial compression tests under plane strain conditions and variable temperature levels.

As can be observed in Fig. 2-b, in case of the simple shear and the uniaxial tensile

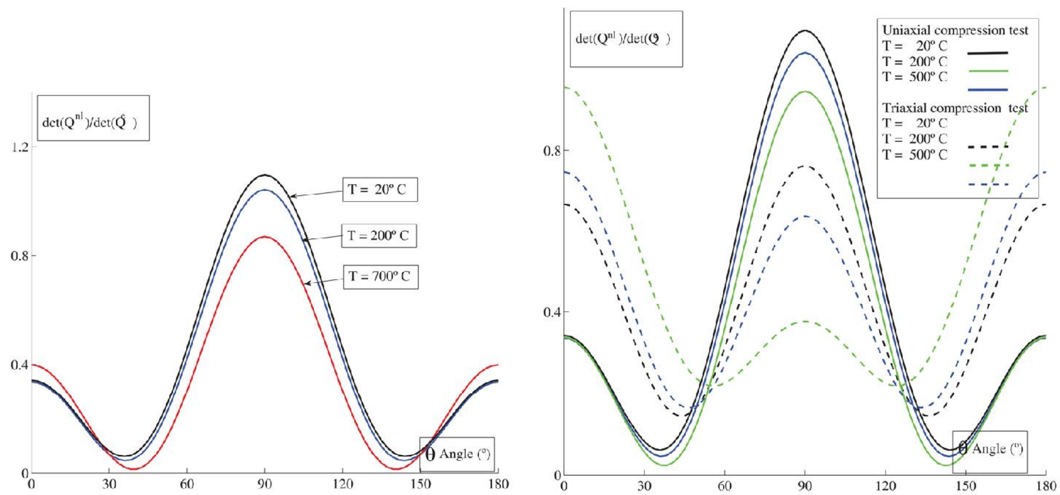

(a) (b)

Figure 3: Numerical localization analysis with the TD-LDP criterion at peak of: (a) the uniaxial compression tests and (b) triaxial compression tests.

tests, failure conditions is fulfilled in the critical directions θ_t= 13° - 167° and θ_s=27° - 153°, respectively, agreeing at 20 and 700°C.

By contrast, in the uniaxial compression test the failure mode turns ductile already, i.e. the localized failure condition is not fulfilled. Regarding Fig. 3-a, for increasing temperature levels from 20° to 700° C, critical localization angles increase from θ_c=33° - 147° to θ_c=40° - 140°, whereas the discontinuous bifurcation conditions are suppressed.

Finally, the influence of the increasing confining pressure in the evolution of failure modes of the TD-LDP material under plane strain conditions and variable temperature levels is numerically analyzed in Fig. 3-b. Localized failure conditions [$\det(Q^{nl})/\det(Q^e)$=0] have been evaluated at peak of the uniaxial and triaxial compression tests satisfying the condition I_1/f'_c= 3, subjected to increasing temperature levels from 20° to 500° C. The results in Fig. 3-b demonstrate the absence of discontinuous bifurcation in the high confinement regime and, moreover, the increment of the positive definition of the localization tensor as well as of the related critical localization angle with the acting confinement and the increment of the temperature level.

6 CONCLUSIONS

The results of the localization analysis in this work demonstrate the capability of the thermodynamically consistent gradient- and fracture energy-based temperature dependent Leon-Drucker Prager (TD-LDP) constitutive model for poroplastic materials to realistically predict both brittle and ductile failure modes of concrete subject to high temperature levels when the governing stress state varies from the tensile and low confinement regime to the high confinement one. Analytical procedures for localized failure evaluations in thermodynamically consistent gradient and fracture energy-based materials have been applied. Numerical analysis of the condition for discontinuous bifurcation are based on the evaluation of the spectral properties of the acoustic or localization tensor through the calculation of its determinant.

The obtained results for the localization analysis under plane strain conditions demonstrate the capabilities of the constitutive model for concrete to reproduce diffuse failure modes in the medium and high confinement regimes as well as localized failure in the tensile regime and its corresponding variations with increasing temperature levels.

In conclusion, the TD-LDP material is able to reproduce the transition from brittle to ductile failure modes of concrete under plane strain conditions when the stress state varies from the tensile to the compressive regime with increasing confinement and temperature levels. The results also demonstrate the capability of the combined gradient and fracture energy-based material theory to realistically reproduce the variation of the critical localization directions with increasing temperature levels, in agreement with the concept that concretes turn more brittle when they are subjected to high temperatures.

REFERENCES

[1] Chan, Y.N. and Peng, G.F. and Chan, J.K.W. Comparison between high strength concrete and normal strength concrete subjected to high temperature. *Mater. Struct.* (1996) **29**: 616-619.

[2] Coussy, O. *Mechanics of Porous Continua*. John Wiley & Sons, (1995).

[3] Etse, G. and Willam, K.J. A fracture energy-based constitutive theory for inelastic behavior of plain concrete. *ACI Mater. J.*, (1994) **120(9)**: 1983–2011.

[4] Etse, G. and Vrech, S. Geometry method for localization analysis in gradient-dependent J_2 plasticity, *J. of Appl. Mech.* (2006), 73: 1026–1030.

[5] Gawin, D. and Pesavento, F. and Schrefler, B.A. Modelling of deformations of high strength concrete at elevated temperatures. *Mater. Struct.* (2004) **37**: 218-236.

[6] Hadamard, J. *Propagation des ondes et les equations d'Hydrodynamique*. New York. Chelsea, (1903).

[7] Hill, R. Acceleration waves in solids, *J. Mech. of Phys. and Sol.* (1962), 1–16.

[8] Hurlbut, B. *Experimental and computational investigation of strain-softening in concrete*. Master's thesis, University of Colorado, (1985).

[9] Mroginski, J.L. and Etse, G. and Vrech, S. M. A thermodynamical gradient theory for deformation and strain localization of porous media. *Int. J. of Plasticity* (2011) **27**: 620-634.

[10] J. Mroginski and G. Etse. A finite element formulation of gradient-based plasticity for porous media with C^1 interpolation of internal variables. *Comput. Geotech.* (2013) **49**: 7–17.

[11] Mroginski, J.L. and Etse, G. Discontinuous bifurcation analysis of thermodynamically consistent gradient poroplastic materials. *Int. J. of Solids and Structures* (2014) **51**: 1834–1846.

[12] Ottosen, S. and Runesson, K. Properties of discontinuous bifurcation solutions in elasto–plasticity. *Int. J. of Solids and Structures* (1991) **27**: 401–421.

[13] Planas, J. and Elices, M. *Towards a measure of G_f: An analysis of experimental results.* F.H. Wittmann, ed. Elsevier, (1986).

[14] Ripani, M. and Etse, G. and Vrech, S. and Mroginski, J. Thermodynamic gradient-based poro-plastic theory for concrete under high temperatures. *Int. J. Plasticity*, (2014) **61**: 157-177.

[15] Svedberg, T. *On the modelling and numerics of gradient-regularized plasticity coupled to damage*, Ph.D. thesis, Chalmers University of Technology. Goteborg, Sweden, (1999).

[16] Ulm, F.J. and Coussy, O. The chunnel fire I: chemoplastic softening in rapidly heated concrete. *J. Eng. Mech.ASCE* (1999) **125**: 272-289.

[17] van Mier, J.G.M. *Strain-Softening of concrete under multiaxial loading conditions.* Ph. D. thesis, Eindhoven University of Technology, Neatherlands, (1984).

[18] van Mier, J.G.M. *Fracture processes of concrete.* CRC Press. (1997)

[19] Vrech, S. and Etse, G. Geometrical localization analysis of gradient-dependent parabolic Drucker-Prager elastoplasticity, *Int. J. of Plasticity* (2006) **22**: 943–964.

[20] Vrech, S. and Etse, G. FE approach for thermodynamically consistent gradient-dependent Plasticity. *Latin Am. Appl. Res.* (2007) **37**: 127–132.

[21] Vrech, S.M. and Etse, G. Gradient and fracture energy-based plasticity theory for quasi-brittle materials like concrete. *Comput. Methods Appl. Mech. Engrg.* (2009) **199**: 136–147.

[22] Vrech, S.M. and Etse, G. Discontinuous bifurcation analysis in fracture energy-based gradient plasticity for concrete. *Int. J. Solids and Structures*, (2012) **49**: 1294–1303.

[23] Willam, K.J. and Etse, G. Failure assessment of the extended Leon model for plain concrete. *SCI-C Conf., Zell and See, Austria,Pineridge Press, Swansea, UK*, (1990). 851–870.